JCTC Journal of Chemical Theory and Computation

Article

pubs.acs.org/JCTC

QM/MM-Based Fitting of Atomic Polarizabilities for Use in Condensed-Phase Biomolecular Simulation

C. Ruben Vosmeer,[†] Ariën S. Rustenburg,[†] Julia E. Rice,[‡] Hans W. Horn,[‡] William C. Swope,[‡] and Daan P. Geerke*,[†]

[†]Leiden/Amsterdam Center for Drug Research, Division of Molecular and Computational Toxicology, Department of Chemistry and Pharmaceutical Sciences, Faculty of Sciences, VU University Amsterdam, De Boelelaan 1083, 1081 HV Amsterdam, The Netherlands

[‡]IBM Almaden Research Center, 650 Harry Road, San Jose, California 95120, United States

ABSTRACT: Accounting for electronic polarization effects in biomolecular simulation (by using a polarizable force field) can increase the accuracy of simulation results. However, the use of gas-phase estimates of atomic polarizabilities α_i usually leads to overpolarization in condensed-phase systems. In the current work, a combined QM/MM approach has been employed to obtain condensed-phase estimates of atomic polarizabilities for water and methanol (QM) solutes in the presence of (MM) solvents of different polarity. In a next step, the validity of the linear response and isotropy assumptions were evaluated based on the observed condensed-phase distributions of α_i values. The observed anisotropy and low average values for the polarizability of methanol's carbon atom in polar solvents was explained in terms of strong solute−solvent interactions involving its adjacent hydroxyl group. Our QM/MM estimates for atomic polarizabilities were found to be close to values used in previously reported polarizable water and methanol models. Using our estimate for α_O of methanol, a single set of polarizable force field parameters was obtained that is directly transferable between environments of different polarity.

1. INTRODUCTION

Since their emergence in the 1950s and 1960s, classical molecular simulation methods have been successfully applied to study physical, chemical, and biological systems, ranging from pure liquids to large complexes such as proteins and cell membranes.[1,2] The increase of computational power has made possible longer simulation times (on the order of milliseconds)[3,4] for systems and processes of high complexity (involving, e.g., protein activation or membrane transport).[5,6] However, the reliability of molecular simulation outcomes still heavily depends on the accuracy of the description of nonbonded interatomic interactions by the applied potential energy model or *force field*. Most force fields used in biomolecular simulation employ a pairwise additive Coulomb function to describe the electrostatic interactions,[7,8] leaving out electrostatic effects such as electronic polarization.[9] In past decades, several *nonpolarizable* biomolecular force fields (such as Amber,[10−12] CHARMM,[13−15] OPLS,[16−18] and GROMOS[19−21]) have been under constant development and have reached high accuracy in describing thermodynamic and other relevant properties of biomolecular systems. However, the omission of explicitly accounting for electronic polarization may lead to limitations in correctly describing the balance of molecular interactions in environments of different polarity,[22] which plays a key role in determining thermodynamic equilibria typically studied in biomolecular simulation.[2] For example, Oostenbrink et al. showed the difficulty of generating a single set of force-field parameters for condensed-phase protein simulation, resulting in two distinct (nonpolarizable) versions of the GROMOS force field, GROMOS 53A5 and 53A6.[20] As another example, polarizable force fields typically bring clear improvement in correctly describing kinetic and dielectric properties of polar solvents, such as water[23] or N-methyl acetamide.[24]

The inducible dipole (ID) or point polarizable dipole (PPD) model[25−27] and the Drude oscillator (DO) or charge-on-spring (COS) approach[28,29] are two of the most widely applied methods to include explicit electronic polarization in *polarizable* force fields. A third one, designated as the fluctuating charge (FQ) model,[30,31] includes electronic polarization effects by allowing atomic point charge distributions of molecules (or molecular building blocks) to adapt to the external electric field. In contrast, the PPD/ID and DO/COS methods assign an inducible dipole moment $\vec{\mu}_i$ to (heavy) atoms i, which adapts its magnitude and direction in response to the external electric field $\vec{E}_i$, depending on its polarizability α_i. Linear response is usually assumed, and the $\vec{\mu}_i$'s are determined using eq 1.[9,32]

$$\vec{\mu}_i = \alpha_i(4\pi\varepsilon_0)\vec{E}_i \tag{1}$$

In the PPD method, $\vec{\mu}_i$ is represented by a point dipole, whereas the COS method introduces two additional point charges attached by a spring with a force constant directly depending on α_i. In both methods, additional interactions are to be evaluated during simulation (i.e., those involving the introduced dipole moments or point charges, respectively), which raises computational costs when compared to the use of nonpolarizable force fields. In both the COS/DO and PPD/ID models, as well as in the FQ method, an iterative scheme[33,34] (or an extended Lagrangian formalism)[31,35−37] is usually employed to energy minimize (or follow in time) the molecular

Special Issue: Wilfred F. van Gunsteren Festschrift

Received: February 1, 2012
Published: April 27, 2012

Table 1. Literature Values for the Polarizability α and the Dielectric Permittivity ε_S for Selected Polarizable Water (a) and Methanol (b) Models, Together with Experimental (exp) and Theoretical (theor) Estimates

			(a) [H_2O]				
	exp[85]	theor[39]	RPOL[86,87]	TIP4P-FQ[31]	SW-RIGID[23]	POL5/TZ[88]	STR/1[29]
α [10^{-3} nm^3]	1.45	1.41	1.47	1.123	1.47	1.291	1.445
ε_S	78.4		106	79	100	98	143
	exp[85]	theor[39]	SWM4-DP[42]	SWM4-NDP[89]	STR/RF[34]	COS/B2[34]	COS/G2[79]
α [10^{-3} nm^3]	1.45	1.41	1.042	0.978	1.445	0.93	1.255
ε_S	78.4		79	79	127	122	88
			(b) [CH_3OH]				
		exp[76]	theor[39]		CHARMM-DO[44]		COS/M[55]
α_{mol} [10^{-3} nm^3][a]		3.32	3.26		2.0		1.32
α_C [10^{-3} nm^3]					1.0		
α_O [10^{-3} nm^3]					1.0		1.32
ε_S		32.6			30.1		31.1

[a] α_{mol} refers to the molecular polarizability of methanol and was obtained for the CHARRM-DO and COS/M models from the sum of the atomic polarizabilities α_C and α_O for carbon and oxygen, respectively.

charge distributions (in the FQ model), induced dipole moments (PPD/ID method), or the positions of the Drude particle (charge-on-spring) due to the external electric field. Typically, the use of an iterative scheme leads to an additional increase in computational costs by a factor of 2−3 in simulations employing the COS model (when compared to simulations with nonpolarizable force fields), because this is the number of iterations usually needed to obtain convergence.[34] The assignment of low fictitious masses to the additional degrees of freedom commonly introduced in extended-Lagrangian based methods (i.e., to the inducible dipoles, Drude particles, or charge distributions) may require the use of smaller time steps in simulation. However, the use of low temperature baths to separately couple the Drude particles has been additionally introduced,[31,38] which makes a decrease in the time step not necessary anymore.

Compared to nonpolarizable force fields, the α_i's are additional parameters to be calibrated along with the nonbonded parameters, which usually need recalibration upon introducing polarizabilities. Initial guesses for atomic polarizabilities are typically derived from gas-phase estimates for molecular polarizabilities (using additive rules, see for example refs 39 and 40) or from fitting atomic dipole moments to best describe the quantum-mechanically determined change in the molecular electrostatic potential upon introducing an external electric field.[41] From previous polarizable force field parametrization studies, it is known that the use of gas-phase estimates for α_i's typically leads to overpolarization (too large values for and fluctuations in molecular dipole moments) in simulations of condensed-phase systems.[34,42−44] For selected polarizable models for liquid water and methanol, Table 1 compares model parameters and calculated dielectric permittivities (ε_s) with gas-phase and experimental estimates, respectively. Note that only two methanol force fields were included in Table 1, because several other parametrization efforts of polarizable methanol models do not report dielectric permittivities.[45−48] Only models presented in Table 1 for which α_i's sum up to significantly lower values for the molecular polarizability (when compared to its gas-phase estimate) show calculated ε_s values close to experimental values. Pauli exclusion effects[42] and local variations in electric field within the solute's molecular volume[49] have been proposed as possible explanations for the need for lower effective polarizabilities for use in the condensed phase, compared to the gas-phase value.

Recently, Kunz and van Gunsteren[50] proposed a polarizable force field for liquid water in which the polarizability of the oxygen atom was made dependent on the magnitude of the electric field at the atom, to allow for damping of the polarization effect at high electric fields. In this way, a polarizable water model (designated as COS/D) could be parametrized with a gas-phase molecular dipole moment *and* polarizability close to the experimentally or theoretically obtained estimates, which simultaneously does not show overpolarization in the condensed phase (as illustrated by the model's dielectric permittivity of liquid water (69.8) being close to the experimental estimate of 78.5).[50] This elegant approach introduces an additional level of complexity by means of two new force-field paramaters to describe the damping effect, and by introducing a dependence of the self-polarization energy term on the local electric field.

In the context of their comprehensive efforts to parametrize the AMOEBA polarizable force field,[51,52] Ponder and co-workers have succeeded in developing parameter sets for water and methanol (as well as for other polar solvents) that correctly describe a wide range of solvent properties, including dielectric permittivities.[52] In AMOEBA, atomic polarizabilities are used on the basis of the QM estimates of Thole,[53] together with the Thole damping model[53] to describe intra- as well as intermolecular damping effects. For this purpose, a damping factor is introduced such that, effectively, molecular polarizabilities are lower than experimental or theoretical gas-phase estimates.[52] In addition, the AMOEBA model includes the use of permanent atomic dipole and quadrupole moments.

For the sake of simplicity, most polarizable force fields for polar liquids such as water and methanol rely on linear polarization (eq 1) and on the use of partial atomic charges only to describe static electrostatic interactions. To parametrize such models, gas-phase estimates of atomic polarizabilities have to be carefully scaled down based on condensed-phase simulation results. In this way, parameter sets can be obtained that reproduce relevant thermodynamic and kinetic properties of the liquids while circumventing overpolarization (as illustrated by the agreement between calculated and experimental values for ε_s, see Table 1). Parametrization based on condensed-phase simulations usually relies on trial-and-error

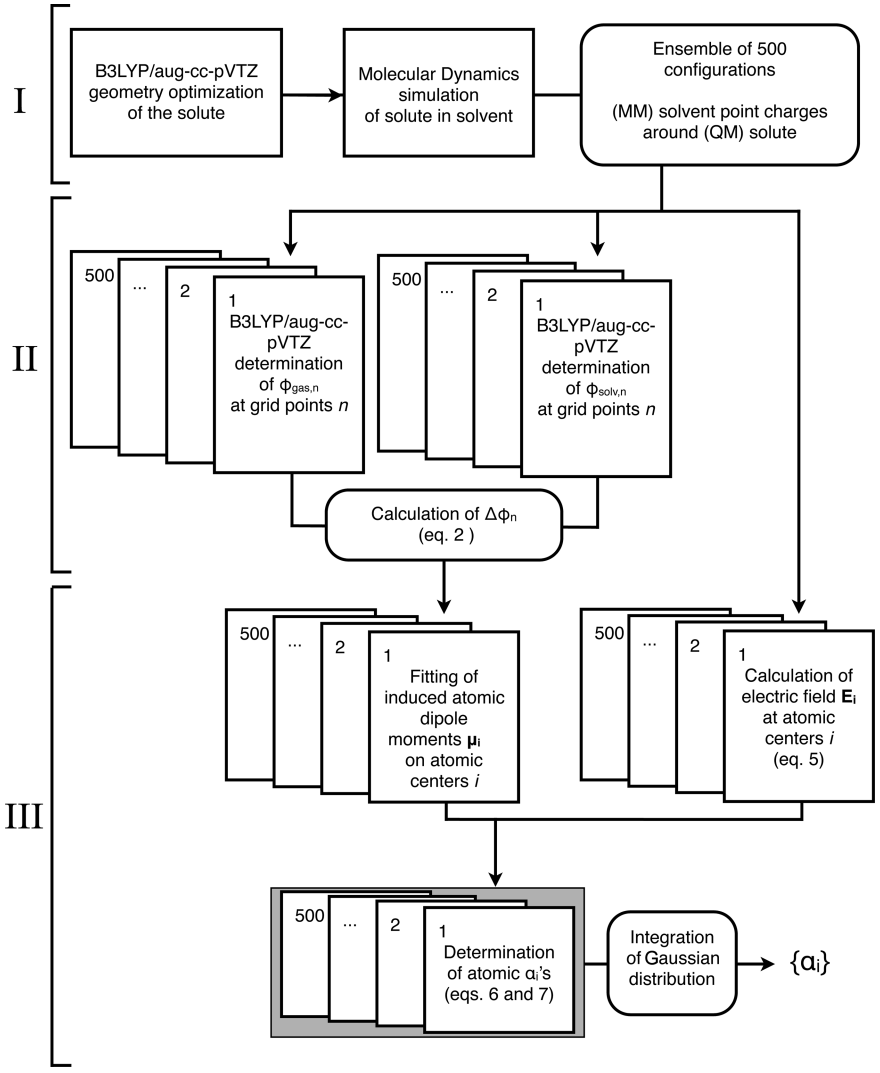

Figure 1. QM/MM-based scheme to obtain (sets of) atomic polarizabilities α_i that best reproduce the response of the solute's electron configuration to its environment in the condensed phase. Latin numbering refers to the latin numbering adopted in section 2.1.

procedures and can be an elaborate task. In addition, polarizabilities for different atom types may require different scaling factors, which may in turn depend on the local molecular environment.[54]

In the current work, we have evaluated the use of a combined QM/MM-based approach to estimate appropriate values for atomic polarizabilities for use in condensed-phase simulations. For an ensemble of (MM) solvent configurations around a (QM) solute as obtained from classical simulation, DFT calculations are performed to determine the response of the solute's electron configuration to the electric field generated by the solvent point charges. For every solvent configuration, atomic dipole moments are fitted that best reproduce the accompanying change in electrostatic potential around the solute. From the fitted dipole moment $(\vec{\mu}_i)$ and electric field $(\vec{E}_i)$ at the atomic centers i and by assuming linear response, the atomic polarizabilities α_i that best reproduce the response in electron configuration are determined.

The use of a fitting scheme for induced atomic dipole moments distinguishes our QM/MM approach from the work of Schropp and Tavan,[49] who recently investigated the response of the dipole moment of a QM (water) solute in an ensemble of MM (water) solvent molecules to estimate a condensed-phase value for its molecular polarizability. In the current work, we have determined which set of atomic polarizabilities best describes the induced dipole moment for a methanol (as mimic of the simplest of the polar amino acid side chains) and a water solute in aqueous environment, as well as for a methanol solute in solvents of medium (methanol) and low (chloroform) polarity. In addition, we evaluate the validity of assuming linearity in and isotropy of the atomic polarizabilities in these condensed-phase systems. By considering different numbers of polarizable centers (i.e., different numbers of inducible atomic dipole moments) to mimic the response of the molecular dipole moment to the external electric field due to the solvent point charges, a quantitiative measure has been obtained to determine the optimal number of polarizable atomic centers to describe the induced molecular dipole moment. Interestingly, for methanol in water, we find distributions of optimum α_i values which show maxima close to the values for α_O and α_C as used in the COS/M model of Yu et al.[55] and the DO model of Anisimov et al.[44] These polarizable models contain one (at O) and two (at C and O) polarizable centers, respectively, and were carefully calibrated based on condensed-phase properties. Thereby, special van der Waals parameters were introduced to describe the methanol interactions with water molecules. Here,

we show that by using our QM/MM estimate for α_O, a polarizable methanol model could be obtained using a single set of force-field parameters that is directly transferable between environments of different polarity.

2. COMPUTATIONAL DETAILS

2.1. QM/MM Based Atomic Polarizabilities. As shown in Figure 1, our approach for the condensed-phase fitting of atomic polarizabilities for the two solutes considered (water and methanol) consists of three consecutive steps:

I. generation of solvent configurations
II. determination of the change in the external electrostatic potential of the (QM) solute due to the electric field generated by the (MM) solvent
III. fitting of the atomic polarizabilities α_i

2.1.1. Generation of Solvent Configurations. During the generation of the ensemble of solvent configurations around the solute, the solute's molecular geometry was kept constrained to its gas-phase optimized geometry, to enable direct comparison between the solute's external electrostatic potential in the gas and condensed phase (step II). The gas-phase optimized geometries of water and methanol were obtained from DFT calculations at the B3LYP level of theory[56−58] using Dunning's aug-cc-pVTZ basis set[59] and the GAMESS-US software package.[60,61]

The optimized geometries were then used in classical molecular dynamics (MD) simulations to obtain ensembles of solvent configurations around the solutes. The methanol solute was solvated in periodic cubic boxes consisting of 1399 SPC water molecules,[62] 1418 SPC/E water molecules,[63] 642 methanol molecules (described by the B3 force field of Walser et al.[64]), 629 methanol molecules (described by the Kirkwood−Buff (KB) force field of Weerasinghe and Smith[65]), or 335 chloroform molecules (described by the force field of Tironi and van Gunsteren[66]). The SPC solute was solvated in a cubic box containing 999 SPC solvent molecules; the SPC/E solute was solvated in 985 SPC/E solvent molecules. For this purpose, the solute was solvated in pre-equilibrated cubic boxes with minimal box lengths of 3.0 nm (with a box volume corresponding to the reported liquid density of the solvent model used), after which all solvent molecules were removed that showed atomic overlap within 0.23 nm of any of the solute atoms. In the MD simulations, the water solute was described by either the SPC or the SPC/E model and the methanol solute was described by either the GROMOS 53A5 or 53A6 parameter set of Oostenbrink et al.[20] Aliphatic hydrogen atoms of the methanol solute were included as dummy atoms during simulation.

After steepest-descent energy minimization, initial atomic velocities were randomly assigned from a Maxwell−Boltzmann distribution (corresponding to a temperature of 300 K). In the MD simulations, Newton's equations of motion were integrated using the leapfrog algorithm,[67] with a time step of 2 fs. An equilibration run of 0.5 ns was followed by 0.5 ns of production, during which atomic configurations were written out every picosecond, yielding in total 500 configurations for every system considered for further use in the QM/MM and fitting protocols (steps II and III). During the simulations, the temperature was kept constant at 300 K using a Berendsen thermostat[68] with a coupling time of 0.1 ps. Only in the simulations with methanol as a solute, was the pressure also kept constant (at 1 atm) using a Berendsen barostat,[68] with a coupling time of 0.5 ps and an isothermal compressibility set to 4.575×10^{-4} $(\text{kJ·mol}^{-1}\text{·nm}^{-3})^{-1}$. In the simulations involving the water solute, the solute was positionally constrained using a molecular orientation as depicted in Figure 2A, to facilitate the analysis of the individual components of the fitted polarizabilities (see section 2.1.3). The system's volume of the pure water simulations was kept constant to a value corresponding to the equilibrium density of the solvent model employed (971 and 997 kg·m^{-3} for SPC and SPC/E, respectively). Geometries of the solvent molecules and of the methanol solute were constrained by keeping interatomic distances constant using the SHAKE algorithm,[69] with a geometric tolerance of 10^{-4}. Nonbonded interactions within a short-range cutoff of 0.8 nm were evaluated every time step, from a grid-based pair list that was updated every five time steps. Interactions between 0.8 and 1.4 nm were calculated every fifth time step as well and kept constant in between. Beyond the long-range cutoff of 1.4 nm, a reaction field correction[70] was applied, using a dielectric constant of 61.0.[71]

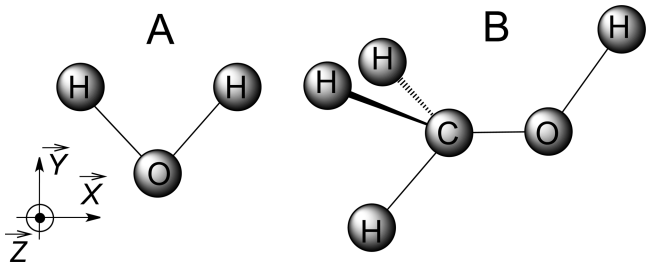

Figure 2. Molecular orientation of (A) the water solute during molecular dynamics (MD) simulations and (B) the methanol solute after rotational fitting of the MD configurations.

2.1.2. Determination of the Change in the Solute's External Electrostatic Potential Due to the Solvent's Electric Field. Solvent configurations as generated during the MD simulation were subsequently prepared for DFT calculations to determine the grid-based external electrostatic potential around the solute in the absence (ϕ_{gas}) and in the presence (ϕ_{solv}) of the solvent molecules. Only those solvent molecules are kept for which the oxygen (of water and methanol solvent molecules) or carbon atom (of chloroform) is within 1.4 nm of any of the solute atoms. Atomic positions for these solvent molecules and the corresponding partial charges are stored as MM input in the DFT/MM calculations of ϕ_{solv}. First, configurations obtained for the systems with methanol as a solute are rotated such that it adapts a molecular orientation as depicted in Figure 2B. Subsequently, a Connolly grid[72] of four layers is defined around the water and methanol solutes, using default GAMESS-US values for the atomic radii, distances between layers that are set to 0.2 times the applied Lennard-Jones radii, and a density of 50 au^{-2}. Values for the electrostatic potential at the grid points were determined at the B3LYP level of DFT,[56−58] using the aug-cc-pVTZ basis set.[59] The B3LYP/aug-cc-pVTZ level of theory was used because it has been shown to give dipole and quadrupole moments close to experimental values for small molecules[73] and a gas-phase value for the polarizability of methanol that is within 0.13×10^{-3} nm^3 from experimental values.[74] External potentials were calculated using a special version of the GAMESS-US software,[60,61] which was adapted to enable electrostatic potential calculations with inclusion of point charges with noninteger and negative values.

Direct contributions of the MM point charges to ϕ_{solv} were not included. The difference $\Delta\phi$ (eq 2) was used to fit the induced atomic dipoles that best describe the response of the wave function to the configuration of solvent molecules (step III).

$$\Delta\phi = \phi_{solv} - \phi_{gas} \tag{2}$$

2.1.3. Fitting of Atomic Polarizabilities. For every system and for every solvent configuration, sets of induced atomic dipole moments $\vec{\mu}_i$ were determined from a least-squares fitting procedure in which the squared difference χ^2 between the QM/MM-determined induced external electrostatic potential $\Delta\phi$ (eq 2) and the external electrostatic potential ϕ_μ from the induced atomic dipole moments was minimized:

$$\chi^2 = \sum_n (\Delta\phi_n - \phi_{\mu,n})^2 \tag{3}$$

In eq 3, summation goes over the Connolly grid points n for which $\Delta\phi$ was estimated, and $\phi_{\mu,n}$ is the electrostatic potential due to the fitted induced dipole moments at n:

$$\phi_{\mu,n} = \sum_i \frac{1}{4\pi\varepsilon_0}\frac{\vec{\mu}_i\cdot\vec{r}_{in}}{r_{in}^3} \tag{4}$$

where $\vec{r}_{in}$ is the vector connecting the grid point n and atomic center i, and r_{in} is its norm. By calculating the electric field $\vec{E}_i$ at the atomic centers due to the point charges q_m of the solvent atoms m,

$$\vec{E}_i = \sum_m \frac{q_m}{4\pi\varepsilon_0}\frac{\vec{r}_{im}}{r_{im}^3} \tag{5}$$

(with $\vec{r}_{im}$ the vector connecting i and m and r_{im} the distance between i and m), and by assuming linear response (eq 1), the atomic polarizabilities α_i that best reproduce the response of the solute's electron configuration to the solvent's electic field can be determined. For this purpose, it is assumed that off-diagonal elements of the polarizability tensor are zero, which is for the considered solutes probably true when averaging over the ensemble of solvent configurations. A three-dimensional vector with elements

$$\alpha_{i,k} = \frac{\mu_{i,k}}{E_{i,k}} \tag{6}$$

is thus determined (where $k = x,y,z$). From a comparison between the x, y, and z elements, a measure for the (an)isotropy of the α_i's can be obtained. Assuming isotropy, $\alpha_{i,x}$, $\alpha_{i,y}$, and $\alpha_{i,z}$ can be averaged to obtain a value for α_i for use in eq 1:

$$\alpha_i = \frac{\alpha_{i,x} + \alpha_{i,y} + \alpha_{i,z}}{3} \tag{7}$$

For the ensemble of solvent configurations, a distribution of atomic polarizabilities is thus obtained, which requires additional averaging to obtain a single value for α_i for use in simulation. For this purpose, a Gaussian curve was fitted to the distribution of α_i values, from which a mean value was obtained corresponding to the α_i value for which the integral over the Gaussian sums up to half of the total integral. For the systems considered, this value was found to be within 0.02×10^{-3} nm^3 from the location of the maximum of the Gaussian.

2.2. Parametrization of a Polarizable Methanol Force Field. Using our condensed-phase estimates for the α_i's and using point-charges based on fitting to the gas-phase external electrostatic potential of methanol at the B3LYP/aug-cc-pVTZ level of theory, a united-atom polarizable force-field parameter set was optimized to reproduce in simulation experimental values for the density ρ and heat of vaporization ΔH_{vap} of the pure liquid. The charge-on-spring (COS) approach was used to include electronic polarizability effects,[28,29,34,75] by assigning atomic polarizabilities to methanol's carbon and oxygen atom.

A cubic box with a box length of 3.2624 nm was filled with 512 methanol molecules, resulting in a density of 784.6 kg m^{-3}, which is within 0.3% of the experimental density of methanol at 298.15 K and 1 atm.[76] Molecular dynamics simulations were performed under NpT conditions using the GROMOS96 package,[19,77] modified to incorporate the use of the COS model.[34,75] Geometries of all molecules were kept rigid using the SHAKE algorithm,[69] with a relative geometric tolerance of 10^{-4}. The temperature was weakly coupled[68] to a bath of 298.15 K with a relaxation time of 0.1 ps. The pressure was weakly coupled[68] to a bath of 1 atm with a relaxation time of 0.5 ps, and the isothermal compressibility was set to 7.513×10^{-4} (kJ mol^{-1} nm^{-3})$^{-1}$. Newton's equations of motion were integrated using the leapfrog algorithm[67] with a time step of 2 fs. Triple-range cutoff radii of 0.8 and 1.4 nm were used to treat van der Waals and electrostatic interactions. Interactions within the first cutoff range were calculated every time step. Intermediate range interactions were evaluated every fifth time step, coinciding with the update of the pair list. Long-range electrostatic interactions beyond the cutoff were represented by a reaction field[70] using model parameters for ε_{RF} of 32.6 for simulations of pure methanol,[55] 4.81 for simulations in chloroform,[78] and 78.5 for simulations in COS/G2 water.[79] At the start of every simulation, initial velocities were assigned from a Maxwell−Boltzmann distribution at the given temperature. For simulations of the pure methanol liquid, 50 ps of equilibration was followed by 500 ps of production from which the enthalpy of vaporization (ΔH_{vap}), the density (ρ), the self-diffusion coefficient (D), the heat capacity (C_p), the isothermal compressibility (κ_T), and the static dielectric permittivity (ε_S) were calculated, using methods described in ref 80. To calculate C_p, two additional NpT simulations at 273 and 313 K were performed. To calculate κ_T, three additional NVT simulations were performed with ρ set to 737, 787, and 837 kg m^{-3}. ε_S was calculated from 10 separate simulations of 6 ns each to obtain a converged average. In all simulations, atomic configurations were written out every 1.0 ps, and energies every 0.2 ps.

Heats and volumes of mixing of our methanol model with COS/G2 water[79] were evaluated by simulating aqueous mixtures at compositions given in Table 2, using equations

Table 2. Mixture Compositions[a] in Simulations of Aqueous Methanol Mixtures at Different Mole Fractions of Methanol (χ_{MeOH})

	χ_{MeOH}				
	0	0.25	0.5	0.75	1
N_{H_2O}	1000	1500	1085	500	0
N_{MeOH}	0	500	1085	1500	512
r_B (nm)	3.10	4.24	4.69	4.85	3.26

[a] N_{H_2O} refers to the number of water molecules and N_{MeOH} to the number of methanol molecules, and r_B is the box length of the cubic periodic box containing the mixtures.

dx.doi.org/10.1021/ct300085z | J. Chem. Theory Comput. 2012, 8, 3839−3853

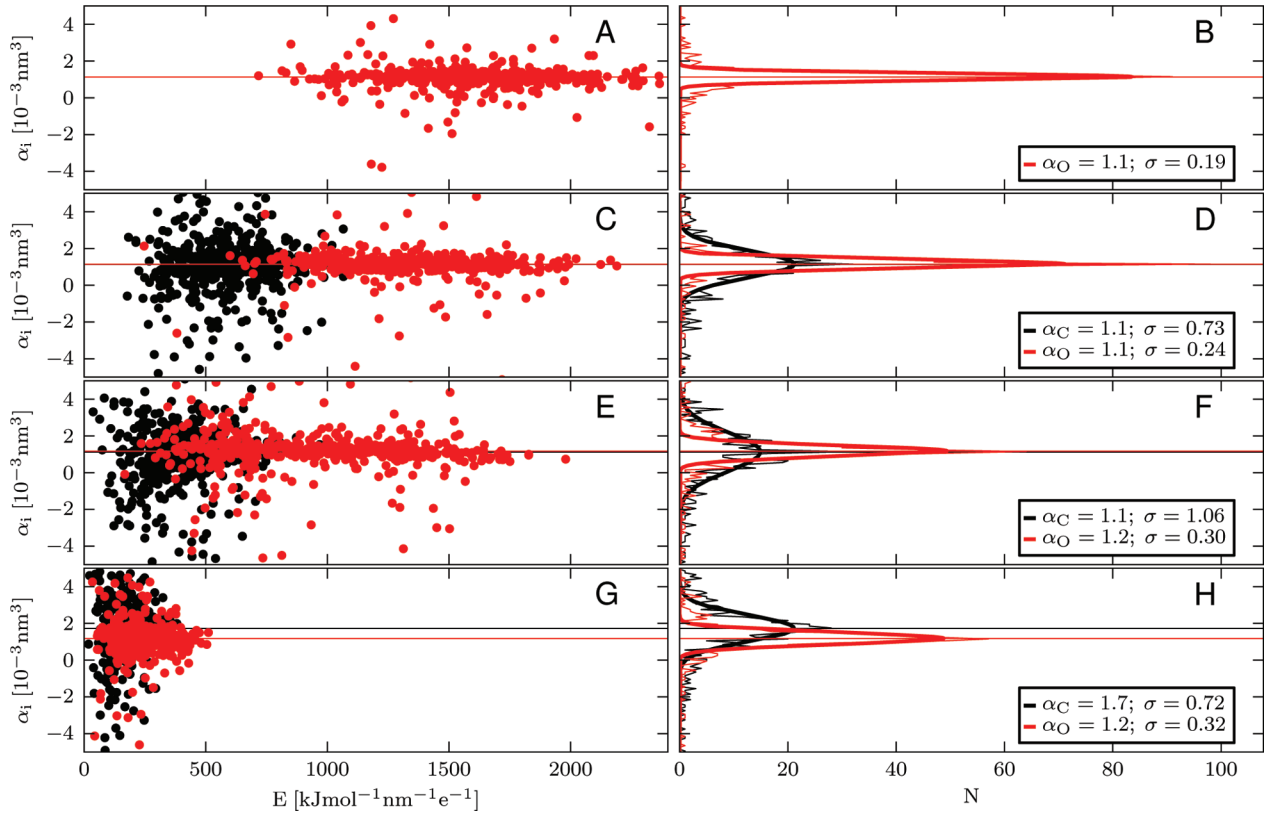

Figure 3. QM/MM determination of atomic polarizabilities α_i (as obtained from electric fields $\vec{E}_i$ and fitted atomic dipole moments $\vec{\mu}_i$ at atomic centers *i*, using eqs 6 and 7), for 500 configurations taken from MD simulations of (A, B) a water solute in water (described by the SPC model), (C, D) a methanol solute (described by the GROMOS 53A6 force field in MD) solvated in SPC water, and (E−H) a methanol solute (described by the GROMOS 53A5 force field in MD) solvated in (E, F) B3 methanol and (G, H) chloroform. To fit the $\vec{\mu}_i$'s, one polarizable center was assigned to the water solute (oxygen) and two polarizable centers to the methanol solute (oxygen and carbon). Panels A, C, E, and G show the correlation between the fitted polarizabilities and the size of the electric field at i. Panels B, D, F, and H show counted distributions of α_i (thin lines) and Gaussian curves fitted to these distributions (thick lines), which were used to obtain, at half the integral of the Gaussian curve, the mean values of α_i (in 10^{-3} nm^3), which are together with the Gaussian standard deviation σ given in the legend boxes. Horizontal lines are drawn in all panels at the mean values of α_i to guide the eye. α_i values and distributions are given in red for water's and methanol's oxygen and in black for methanol's carbon atom.

given in ref 55. No additional parameters were used to describe water−alcohol interactions. Configurations as well as energies of the mixtures were written out every 0.2 ps. ε_{RF} was a linear combination of the ε_{RF} values of COS/G2 and our methanol model, as a function of the mole fraction. To evaluate the quality of the model further, the free energy of hydration (ΔG_{hydr}) and the free energy of solvation in chloroform ($\Delta G_{solv,CHCl_3}$) were calculated from simulations using the methodology and settings given in ref 22. For chloroform, the COS/C model of Lin et al.[78] was used.

3. RESULTS AND DISCUSSION

Figure 3, panels A and B present results for our QM/MM based fitting of α_i at water's oxygen atom for configurations of a QM solute in MM water, by using the SPC water model[62] in the MD simulations to generate the configurations. Use of the SPC/E model[63] (which has both a higher density and molecular dipole moment than SPC water) for either the solute, solvent, or both, was found to neither qualitatively nor quantitatively change the following discussion. Figure 3, panel A shows that α_i values are clustered around a constant value, independent of the size of the local electric field at the oxygen atom. This indicates that linear response (eq 1) is a suitable approach to describe electronic polarization effects in an aqueous environment, which is confirmed by Figure 4 (panels A−C), which demonstrates the obtained linear correlation between the separate vector elements of the fitted dipole moments and electric fields at the solute's oxygen (with a correlation coefficient R^2 being higher than 0.9).

Figure 3, panel B presents the number distribution of α_i values obtained for the water solute in SPC water. A Gaussian curve was fitted to this distribution, from which a mean value for α_i of 1.1×10^{-3} nm^3 was obtained. This value is close to the value used in polarizable water models for which dielectric permittivities have been reported that are close to the experimental estimate (Table 1). It is also close to the mean value of 1.08×10^{-3} nm^3 obtained by Schropp and Tavan in their DFT/MM study on the optimal value for the molecular polarizability in TIP3P and TIP4P water,[49] confirming the validity of our settings and approach. In the remaining, we will study the electronic polarizability of a methanol solute (as a mimic of the simplest polar amino acid side chain) in environments of different polarity.

3.1. Fitting of Atomic Polarizabilities for a Methanol Solute. Inducible dipole moments were fitted to best reproduce the change $\Delta\phi$ (eq 2) in the external electrostatic potential of methanol due to the fields of point charges in water, methanol, and chloroform solvent configurations, as determined at the B3LYP/aug-cc-pVTZ level of theory. Fitting to $\Delta\phi$ of the inducible solute dipole moments was performed

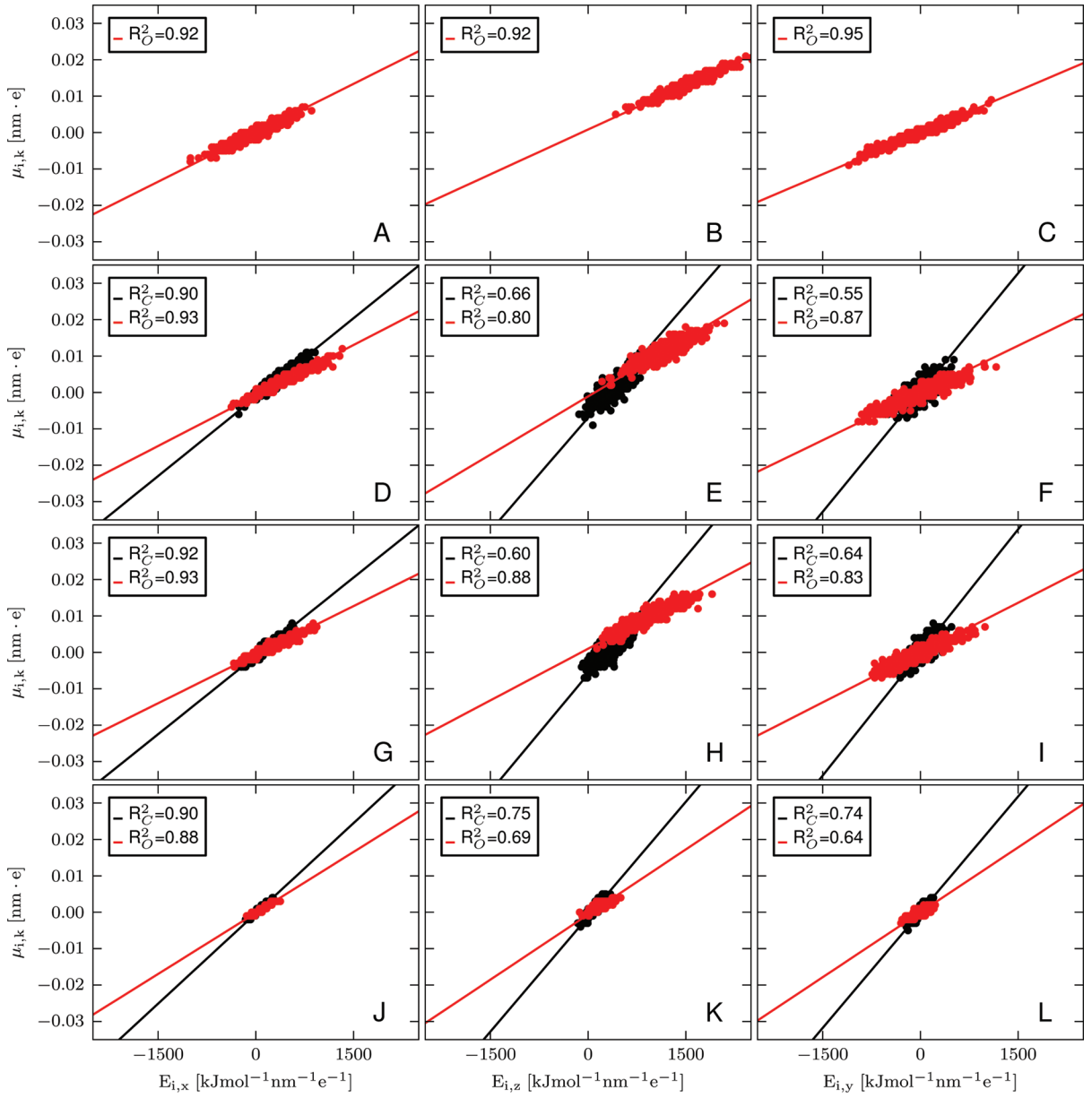

Figure 4. Correlation between x (panels A, D, G, and J), y (panels B, E, H, and K), and z (panels C, F, I, and L) elements k of fitted dipole moments $\vec{\mu}_i$ and of electric fields $\vec{E}_i$ at atomic centers i (oxygen, red; carbon, black) of a water (panels A–C) and a methanol solute (panels D–L), for ensembles of 500 solvent configurations obtained in SPC water (panels A–F), B3 methanol (panels G–I), and chloroform (panels J–L). Solid lines present linear fits for the obtained correlation between $\mu_{i,k}$ and $E_{i,k}$; the corresponding correlation coefficient R^2 is given in the legend boxes.

by assigning either a single inducible dipole moment (to the oxygen atom), two inducible dipole moments (to both heavy atoms C and O), or three inducible dipole moments (to the carbon, oxygen, and hydroxyl hydrogen atom). Most polarizable force fields assign inducible dipole moments to heavy atoms only. Panels C–H of Figure 3 present distributions of C and O polarizabilities determined from the fitted dipole moments at these two centers, in the three solvents considered. The results for methanol in water as presented in Figure 3, panels C and D were generated from MD simulations using the GROMOS 53A6 force field[20] (optimized to describe hydration free energies of polar amino acid side chains in SPC water) to represent the solute, in combination with the SPC model for water.[62] Distributions shown in Figure 3, panels E and F are based on MD simulations of methanol with GROMOS 53A5 solute parameters[20] (optimized based on thermodynamic properties of pure liquids for the polar amino acid side chain moieties) and the B3 methanol solvent model of Walser et al.[64] Because of the possible influence of force-field parameters on thermodynamic and structural properties,[64,65] the effect of using different force fields to generate solvent configurations on the fitted dipole moments and atomic polarizabilities was evaluated by comparing results generated from simulations using either GROMOS 53A5 or 53A6 solute parameters, either the SPC or SPC/E[62,63] water model, and either the methanol B3 or KB solvent models.[64,65] Similar distributions for atomic polarizabilities were obtained when comparing results based on the use of different force-field parameter sets. This is reflected in Figure 5 by the small differences in the mean values for the obtained distributions. The largest differences in mean α_i values due to the use of different force-field parameter sets were observed between the use of either the B3 or KB solvent

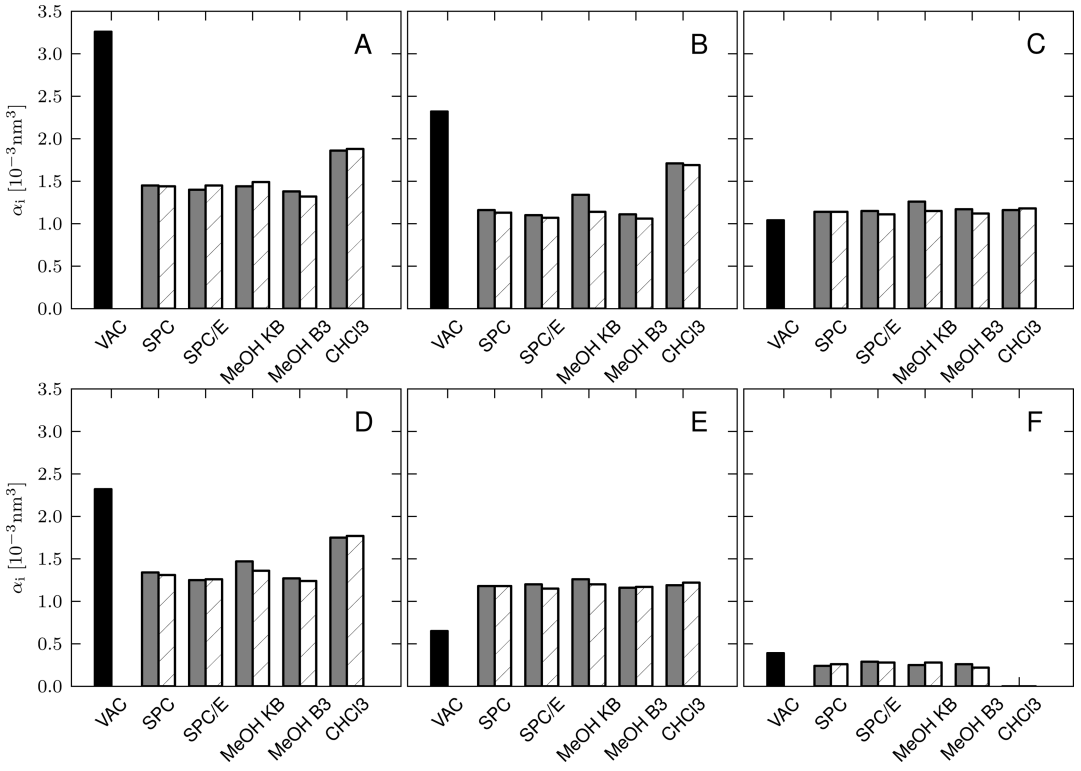

Figure 5. Vacuum estimates (black bars) for atomic polarizabilities α_i, as well as (averaged) values for α_i for a methanol solute in water (described by the SPC or SPC/E model), methanol (described by the KB or B3 model), or chloroform, as obtained from our QM/MM approach from MD simulations using GROMOS 53A5 (gray bars) or 53A6 (hashed bars) to describe the solute. α_i values in panel A are obtained by fitting a single atomic polarizability (on methanol's oxygen). α_i values in panels B and C are obtained by fitting on two atomic sites (on methanol's carbon (B) and oxygen (C)), and the α_i values in panels D−F are obtained by fitting on three centers (carbon (D), oxygen (E), and hydrogen (F)). Vacuum estimates are the sum of gas-phase atomic polarizabilities (taken from ref 39), for all atoms (panel A), for the methyl group (panels B and D), for the hydroxyl group (panel C), or for the oxygen atom (panel E) or hydrogen atom only (panel F).

models in the pure methanol simulations, especially when comparing the results for the carbon atom (Figure 5, panels B and D). In this case, the widest of all distributions was obtained (with a width of the fitted Gaussian being on the same order as the integrated value, see Figure 3, panel F). As a result, the effect of the force field on differences in obtained α_i values and distributions was not found to affect the discussion in the remainder of this section. Note that on the basis of a comparison of the obtained atomic α_i's for methanol in water (when using either GROMOS 53A5 or 53A6 parameters for methanol and either the SPC or SPC/E solvent model), we do not expect that explicit inclusion of MM polarization in our MD simulations and in the QM/MM electrostatic potential calculations will significantly affect the results of the polarizability fitting. Both the SPC and SPC/E water models and the GROMOS 53A5 and 53A6 methanol parameters differ with respect to the size of their atomic partial charges (and consequently, their molecular dipole moments).[20,63] This difference between the methanol models effectively accounts for differences in molecular polarization to best describe nonbonded interactions of the methanol solute with either methanol (53A5) or water (53A6) solvent molecules.[20] Similarly, the difference in point charges between the SPC and SPC/E water models effectively accounts for the self-polarization energy of the water solvent molecules.[63] Because of these substantial differences in the (implicit) account for polarization effects in both pairs of force-field parameter sets, and because use of any combination of parameter sets for the methanol solute in water led to similar results in the fitted atomic polarizabilities (especially at methanol's oxygen atom, see Figure 5), we do not expect that explicit inclusion of MM polarization will significantly change the outcomes of our QM/MM based fitting scheme.

Figure 3, panels C and E show that values for α_O cluster around its mean value, independent of the size of the electric field at O. This indicates that also for methanol's oxygen atom in polar environment, linear response of its inducible dipole moment can be assumed. The linear correlation between the x, y, and z components of the fitted dipole moments and of the electric fields at methanol's oxygen (with $R^2 > 0.8$, see Figure 4, panels D−I) confirms the validity of this assumption.

For α_C (as well as for α_O in the apolar chloroform environment), the linear behavior over the range of E_i values is less obvious, considering the large spread in fitted values in Figure 3, panels C−H. In addition, the occurrence of negative values for α_i seems unphysical. It should be realized however that the α_i's ($\vec{\mu}_i$'s) are effective parameters (descriptors) to describe the total response of the solute's electronic configuration to the external electric field. As such, it also accounts for changes in quadrupole and higher multipole moments of the solute. This might explain why negative α_i's are especially observed for carbon and when using more than one polarizable center. Whereas the inducible dipole moment at O may predominantly account for the change in overall molecular dipole moment, the fitted $\vec{\mu}_C$ may well adopt opposite direction, to effectively induce a quadrupole moment in order to further improve the fit. Despite the relatively wide spread in α_C values and the occurrence of negative polarizabilities, also

for carbon (and O in chloroform) correlation was obtained between fitted $\vec{\mu}_i$ and $\vec{E}_i$ components, with R^2 values ranging from 0.55 to 0.92 (Figure 4, panels D−L).

From Figure 3, panels C and E, it can be seen that in the water and methanol solvents, typical electric fields at methanol's oxygen atom are significantly higher than at the solute's carbon atom. This is not surprising when considering the strong interactions with and directionality of hydrogen bonding solvent molecules toward the oxygen atom. Simultaneously, panels D and F of Figure 3 show a much smaller spread in α_i values for methanol's oxygen than for its carbon atom. A possible explanation for the larger spread in α_i values at small E_i values (also reflected by the α_i distributions for both C and O in chloroform, see Figure 3, panel G) is offered by the fact that the change $\Delta\phi$ in the molecular external potential compared to the gas phase is largely due to strong and directional interactions of solvent molecules with the solute's hydroxyl group. Therefore, the change in electron configuration around the carbon atom may well depend on the strength of solute−solvent hydrogen bonding interactions and the resulting intramolecular polarization, instead of on the electric field due to the solvent at the methyl group itself. This is confirmed by the large components of the fitted α_C polarizabilities along the C−O bond ($\alpha_{i,x}$), see section 3.2. In other words, intramolecular interactions may well be dominant in polarizing the apolar CH_3 group, whereas use of the external electric field in eq 1 rather implies that electronic polarization effects are depending on intermolecular interactions. The resulting scattering in α_C values leads to a significant reduction in the obtained mean value for α_C, when compared to the gas-phase estimate of Miller[39] or Anisimov et al.[44] of 2.3×10^{-3} nm^3 and 1.9×10^{-3} nm^3, respectively (Figure 5, panels B and D). This effect is stronger in the hydrogen bonding solvents water and methanol (mean α_C value of 1.1×10^{-3} nm^3) than in chloroform (1.7×10^{-3} nm^3). In conclusion, intramolecular polarization offers an additional explanation for the need of lower values of atomic polarizabilities in the condensed phase compared to gas-phase estimates, which was recently suggested to be due to Pauli exclusion effects,[42] or explained by the observation that for a solute molecule such as water, the electric field at the chosen polarizable center is typically significantly higher than within the remaining part of the molecular volume.[49]

α_O adopts relatively constant values in the solvents of different polarities considered (about 1.1×10^{-3} nm^3, Figure 3). Interestingly, this α_O value as well as our mean α_C value in polar (water, methanol) environment (1.1×10^{-3} nm^3, Figure 3) are close to the value of 1.0×10^{-3} nm^3 as presented for α_C and α_O by Anisimov et al.[44] in their parametrization of DO alcohol models (which started from gas-phase estimates of α_C and α_O, and recalibrated polarizabilities and other force-field parameters based on condensed-phase properties). Similarly, from our QM/MM fitting of a single polarizability at the oxygen to represent the response of the molecular dipole moment to the methanol and water solvents (Figure 5, panel A), we obtained values close to the value used in the COS/M model of Yu et al.[55] (of 1.32×10^{-3} nm^3, Table 1b). We have also fitted induced dipole moments and polarizabilities to $\Delta\phi$ by assigning three polarizable centers (i.e., at C and O as well as the hydroxyl hydrogen atom). Figure 5, panels D−F present mean values obtained from the distributions of the three α_i values in different solvents. The largest spread is again obtained in α_C values, and only small values were obtained for α_H. Because of the increased computational cost and the increased chance of a polarization catastrophe (polar hydrogens often do not carry (repulsive) van der Waals parameters), hydrogen atoms are usually omitted when assigning polarizable centers. Here, we show that use of an additional polarizable center at hydrogen only brings small improvement in describing the response of the molecular electrostatic potential to the field of solvent point charges, when compared to the situation of using polarizabilities at C and O only. Figure 6 presents χ^2 values

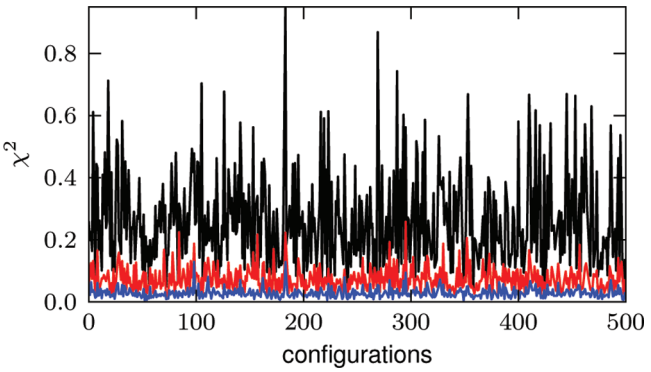

Figure 6. Values of χ^2 for the fitted solvent configurations calculated from eq 3 for fitting of the external electrostatic potential of a QM methanol solute in SPC water, using one (at oxygen, in black), two (at oxygen and carbon, in red), or three (at oxygen, carbon, and hydroxyl hydrogen, in blue) atomic centers to fit induced dipole moments on.

(calculated from eq 3) for the fits of 1, 2, or 3 induced dipole moments on the methanol solute in water. From Figure 6, it can be seen that a significant gain in accuracy (i.e., decrease in χ^2 values) can be obtained when introducing a second polarizable center at the carbon atom. However, the additional decrease in χ^2 values upon introducing a third polarizable center (at the hydroxyl hydrogen atom) is less significant (Figure 6).

3.2. Isotropy of the Obtained Atomic Polarizabilities.

Accounting for anisotropy can enhance the accuracy of the treatment of electronic polarization effects in simulation,[24] but it also needs computationally costly matrix operations and can introduce torques. In the case of water, gas-phase values for the diagonal elements of the polarizability tensor deviate only 4% from their average (isotropic) value,[9] which implies that isotropic treatment of oxygen's polarizability in water is sufficiently accurate. From the condensed-phase distributions for x, y, and z elements of the fitted polarizabilites for water's oxygen atom in aqueous solution (Figure 7, panels A and B), mean values for α_x, α_y, and α_z are obtained that are within 10% of the average value for α_O (of 1.1×10^{-3} nm^3). Moreover, the separate distributions for α_x, α_y, and α_z show significant overlap (Figure 7, panel B), which is an additional validation of assuming isotropy. A similar conclusion can be drawn for fitted α_x, α_y, and α_z values for methanol's oxygen atom (obtained in water) when including a single (Figure 7, panels C and D) or two polarizable centers (Figure 7, panels G and H), although differences between individual α elements and its mean value (of 1.4×10^{-3} nm^3 and 1.1×10^{-3} nm^3, respectively) may sum up to 25% and 15%, respectively. For methanol's carbon atom, large deviations in individual x, y, and z values of the fitted polarizabilities are obtained. Such a large anisotropy in α_C can be understood from the large intramolecular contribution of electronic polarization along the C−O bond, as reflected by the

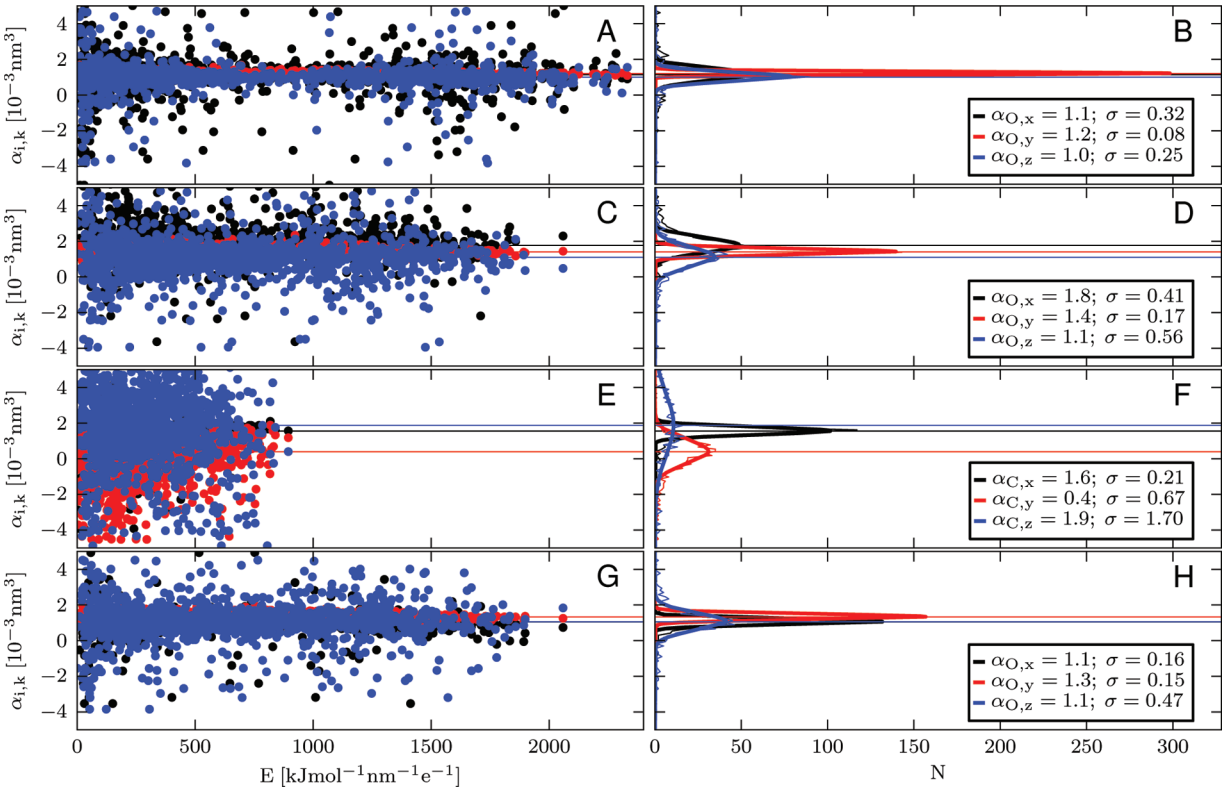

Figure 7. QM/MM determination of *x*, *y*, and *z* components of the atomic polarizability elements $\alpha_{i,k}$ (as obtained from electric fields $\vec{E}_i$ and fitted atomic dipole moments $\vec{\mu}_i$ at atomic centers *i*, using eqs 6 and 7), for 500 configurations taken from MD simulations of (A, B) a water solute in water (described by the SPC model) and (C−H) a methanol solute described by the GROMOS 53A6 force field in MD solvated in SPC water. To fit the $\vec{\mu}_i$'s, one (A−D) or two (E−H) polarizable centers were assigned to the solute (oxygen or oxygen and carbon, respectively). The left panels show the correlation between the fitted polarizabilities and the size of the electric field at *i*. The right panels show counted distributions of $\alpha_{i,k}$ (thin lines) and Gaussian curves fitted to these distributions (thick lines), which were used to obtain, at half the integral of the Gaussian curve, the mean values of $\alpha_{i,k}$ (in 10^{-3} nm^3), which are together with the Gaussian standard deviation σ given in the legend boxes. Horizontal lines are drawn in all panels at the mean values of $\alpha_{i,k}$ to guide the eye. $\alpha_{i,k}$ values and distributions are given in black for the *x* direction, red for the *y* direction, and blue for the *z* direction (as defined in Figure 2).

high value of $\alpha_{i,x}$ for C in Figure 7, panel F. This is probably due to the strong intermolecular (hydrogen bonding) electrostatic interactions involving the hydroxyl group when compared to the small electrostatic fields at the methyl group.

3.3. Use of the Optimal Value for α_O to Parametrize a Polarizable Methanol Force Field. On the basis of the MD simulations in SPC water using the GROMOS 53A6 parameters for the solute, our QM/MM estimate for the condensed-phase fitting of α_O was 1.1×10^{-3} nm^3, which is slightly higher than the gas-phase estimates of 1.0×10^{-3} nm^3 by both Miller[39] and Anisimov et al.[44] This estimate for α_O was used to reparametrize a methanol force field with two polarizable centers. In the parametrization procedure, α_C was treated as an effective, variable parameter because of the large spread in obtained α_C values (Figure 3), the variation in mean values within environments of different polarity (Figure 5), and the differences in the separate $\alpha_{C,x}$, $\alpha_{C,y}$ and $\alpha_{C,z}$ values (section 3.2). Starting from the mean value for α_C determined in water (1.1×10^{-3} nm^3, Figure 3) and from the COS/M van der Waals (vdW) parameters,[55] and by using gas-phase estimates for partial charges and the COS/M methanol geometry, α_C and vdW parameters were varied to obtain methanol models that reproduce experimental values for the heat of vaporization ΔH_{vap} and the density ρ of the pure liquid in simulation. From the various combinations of α_C and vdW parameters reproducing ΔH_{vap} and ρ of the liquid, the parameter set with $\alpha_C = 0.95 \times 10^{-3}$ nm^3 showed a value of the dielectric permittivity ε_S that is close to experimental values, whereas models with a higher α_C still show overpolarization (as indicated by a significant overestimation of ε_S, results not shown). Our final methanol parameter set (with $\alpha_O = 1.1 \times 10^{-3}$ nm^3, $\alpha_C = 0.95 \times 10^{-3}$ nm^3 and gas-phase partial charges) is presented in Table 3 and is designated as CPC. Tables 3 and 4 compare CPC parameters and properties with experimental data and with data for other methanol models that use atomic-centered polarizabilities, including the COS/M model of Yu et al.[55] (which has one polarizable center at O) and the CHARMM-DO model of Anisimov et al.[44] (having two polarizable centers, at C and O). CPC and COS/M both have a fixed geometry and three atomic interaction sites (the only difference in the number of force-field parameters being the number of polarizable centers). The CHARMM-DO model shows a higher degree of complexity in terms of the number of interaction sites (Table 3).

Values for pure-liquid thermodynamic properties of the CPC model are in good agreement with experimental values and show slight improvement over COS/M in terms of the pure-liquid density and heat capacity, and over CHARMM-DO in terms of the isothermal compressibility, see Table 4. Structural properties of the CPC model were compared in terms of the radial distribution functions $g(r)$, both with experimentally derived $g(r)$ data[81,82] and with the local structure in COS/M

Table 3. Values for the Partial Atomic Charges (q), Interatomic Distances (d), Bond Angles ($\angle$), Permanent Dipole Moments (μ_0), Atomic Polarizabilities (α), and van der Waals Parameters (C_6 and C_{12}) for the CPC, COS/M, and CHARMM-DO Polarizable Methanol Models[a]

		CPC	COS/M[b]	CHARMM-DO[c]	exp[d]
q(O)	[e]	−0.55	−0.53	0.00	
q(lp)	[e]			−0.23	
q(H)	[e]	0.34	0.36	0.36	
q(Me)	[e]	0.21	0.17		
q(C)	[e]			−0.14	
q(H_C)	[e]			0.08	
d(O−H)	[nm]	0.1000	0.1000	0.0970	0.095
d(Me−O)	[nm]	0.1430	0.1430		
d(C−O)	[nm]			0.1430	0.142
d(H−Me)	[nm]	0.1988	0.1988		
d(H_C−C)	[nm]			0.1110	0.109
∠C−O−H	[deg]			107.6	108.53
∠H_C−C−O	[deg]			109.9	
∠H_C−C−H_C	[deg]			109.1	108.63
μ_0	[D]	1.80	1.75	1.83	1.70
α_{mol}	[10^{-3}nm^3]				3.32
α_O	[10^{-3}nm^3]	1.100	1.320	1.0	
α_{Me}	[10^{-3}nm^3]	0.950		1.0	
$(C_{12}(O))^{1/2}$	[10^{-3} (kJ·mol^{-1}·nm^{12})$^{1/2}$]	1.475	1.615	1.533	
$(C_{12}(H))^{1/2}$	[10^{-3} (kJ·mol^{-1}·nm^{12})$^{1/2}$]			5.4×10^{-5}	
$(C_{12}(C))^{1/2}$	[10^{-3} (kJ·mol^{-1}·nm^{12})$^{1/2}$]			3.129	
$(C_{12}(H_C))^{1/2}$	[10^{-3} (kJ·mol^{-1}·nm^{12})$^{1/2}$]			0.142	
$(C_{12}(Me))^{1/2}$	[10^{-3} (kJ·mol^{-1}·nm^{12})$^{1/2}$]	5.685	4.400		
$(C_6(O))^{1/2}$	[(kJ·mol^{-1}·nm^6)$^{1/2}$]	0.04720	0.04760	0.03485	
$(C_6(H))^{1/2}$	[(kJ·mol^{-1}·nm^6)$^{1/2}$]			0.00010	
$(C_6(C))^{1/2}$	[(kJ·mol^{-1}·nm^6)$^{1/2}$]			0.04608	
$(C_6(H_C))^{1/2}$	[(kJ·mol^{-1}·nm^6)$^{1/2}$]			0.00737	
$(C_6(Me))^{1/2}$	[(kJ·mol^{-1}·nm^6)$^{1/2}$]	0.11161	0.09421		

[a]O refers to methanol's oxygen atom, lp to virtual lone-pair sites (in the CHARMM-DO model, positioned at a distance of 0.035 nm from the oxygen center), H to the hydroxyl hydrogen atom, Me to the united atom CH_3 group, C to the carbon atom, and H_C to explicit aliphatic hydrogen atoms. The presented van der Waals parameters of the CHARMM-DO model were derived from Lennard-Jones parameters given in refs 44 and 90 (in combination with the potential energy term for Lennard-Jones interactions given in ref 91). [b]Ref 55. [c]Ref 44. [d]Experimental and theoretical values were taken from ref 76.

methanol (Figure 8). This comparison shows a similar match with experimental data when compared to COS/M. However, Table 4 also shows a too low diffusion constant for the CPC model, which makes the CPC model less suited for the description of kinetic properties of the pure liquid but will not affect the thermodynamic properties that drive biologically relevant processes.

Mixing properties of CPC methanol with COS/G2 water[79] were evaluated as well, see Figure 9. Heats of mixing are within 0.4 kJ·mol^{-1}, and volumes of mixing are well within 0.1 mL mol^{-1} from experimental values, which is an excellent match and a further improvement over the performance of COS/M (Figure 9). Note that the maximum error in ΔH_{mix} of 0.4 kJ mol^{-1} (at χ_{MeOH} = 0.75) is well within k_BT (which is 2.5 kJ mol^{-1} at 300 K and can be considered as a measure for typical fluctuations in the kinetic energy of the system). In addition, the computed heat of vaporization of the mixture at χ_{MeOH} = 0.75 is within 1% from the experimental value (which was derived from experimental values for the heat of mixing[83] and the heats of vaporization of liquid water[84] and methanol[76]). Interestingly, no special van der Waals parameters had to be introduced to obtain this match with experimental values for the aqueous mixture properties, whereas such special parameters were previously introduced for COS/M and CHARMM-DO (see refs 55 and 44, respectively). Finally, free energies of solvation of CPC methanol in COS/G2 water and in chloroform (described by the COS/C model of Lin et al.[78]) were computed. Values were obtained within 1.7 kJ mol^{-1} of experimental values (i.e., within k_BT, see Table 4), which validates the use of the CPC parameter set for use in biomolecular simulation, because the balance in interactions in environments of such a different polarity is what usually drives processes of biochemical and -physical interest.[2]

4. CONCLUSION

In the current work, we have used a QM/MM based fitting approach to determine values for atomic polarizabilities for use in condensed-phase (bio)molecular simulation. Ensembles of configurations of (MM) solvent molecules around a (QM) solute were obtained from classical MD simulations, after which induced atomic dipole moments were fitted to mimic the response of the solute's external electrostatic potential to the electric field generated by the solvent point charges (determined at the B3LYP/aug-cc-pVTZ level of theory). Fits were performed by assigning inducible dipole moments to the heavy atoms of a water and a methanol solute, in ensembles of solvent configurations of different polarity (water, methanol, and chloroform solvents). A comparison of the accuracy of the

Table 4. Values for the Density (ρ), Heat of Vaporization (ΔH_{vap}), Self-Polarization Energy ($U_{selfpol}$), Average and Induced Dipole Moments ($\langle\mu_{liq}\rangle$ and $\langle\mu_{ind}\rangle$), Dielectric Permittivity (ε_S), Self-Diffusion Constant (D), Isothermal Compressibility (k_T), Heat Capacity (C_p), Free Energy of Hydration ΔG_{hydr}, and Free Energy of Solvation in Chloroform ($\Delta G_{solv,CHCl_3}$) of Methanol at 298.15 K and 1 atm, Calculated from Simulations Using CPC, COS/M, and CHARMM-DO Polarizable Methanol Models, or Taken from Experiment (exp)

		CPC[a]	COS/M[b]	CHARMM-DO[c]	exp
ρ	[kg·m^{-3}]	794.0	774.6	791.6	786.9[d]
ΔH_{vap}	[kJ·mol^{-1}]	36.8	37.8	37.4	37.4[e]
$U_{self\text{-}pol}$	[kJ·mol^{-1}]	9.12	15.4		
$\langle\mu_{liq}\rangle$	[D]	2.43	2.52		2.87[f]
$\langle\mu_{ind}\rangle$	[D]	0.63	0.80		
ε_S		34.4	31.1	30.1	32.6[e]
D	[10^{-9} m^2·s^{-1}]	1.1	1.7	2.6	2.4[g]
k_T	[10^{-6}·atm^{-1}]	119	129	87[h]	123[e,i]
C_p	[J·mol^{-1}· K^{-1}]	62.5	113		81.1[e]
ΔG_{hydr}	[kJ·mol^{-1}]	−19.6	−19.7	−19.4	−21.3[j]
$\Delta G_{solv,CHCl_3}$	[kJ·mol^{-1}]	−12.6			−13.9[j]

[a]Current work. [b]Ref 55. [c]Ref 44. [d]Ref 92. [e]Ref 76. [f]Ref 93. [g]Ref 94. [h]Value at 313.15 K. [i]Value at 293.15 K. [j]Ref 95.

fitted electrostatic potentials around the methanol solute when fitting at either one (at O), two (at C and O), or three (C, O, and hydroxyl H) atomic centers showed that the use of two polarizable centers in the condensed phase is a good tradeoff in terms of accuracy on one hand and computational costs and risk for the polarization catastrophe on the other hand.

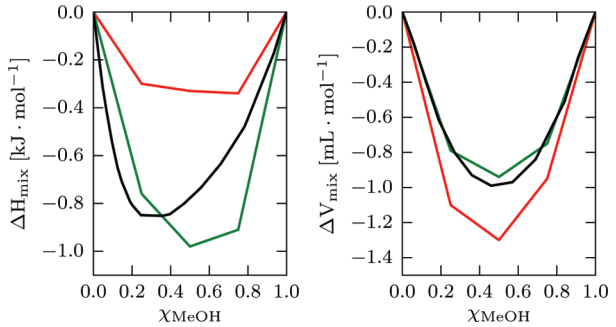

Figure 9. Heat (ΔH_{mix}) and volume (ΔV_{mix}) of mixing of water−methanol mixtures at different methanol mole fractions (χ_{MeOH}) at 300 K and 1 atm, calculated from simulations using the CPC (in green) and COS/M (in red) polarizable models for methanol and the COS/G2 model for water. Experimental values are given as well (in black, taken from refs 83 and 92, respectively).

From the induced atomic dipole moments, effective condensed-phase atomic polarizabilities α_i were derived, by assuming linear response. Using our approach, the linear-response assumption was validated for the polarizable oxygen atom of the water and methanol solute in polar environments (water and methanol solvents). For these atom types, isotropy of the electronic polarization was shown to be a valid approximation as well: the condensed-phase estimates for $\alpha_{i,x}$, $\alpha_{i,y}$, and $\alpha_{i,z}$ elements were within 10−15% of the effective, averaged α_i value. For atoms exposed to relatively low electric fields (such as the carbon atom of the methanol solute and the oxygen atom in chloroform), validation of assuming isotropy and linear response was less obvious, because wide distributions of fitted atomic polarizabilities were obtained in these cases. The relatively large anisotropy in obtained $\alpha_{i,x}$, $\alpha_{i,y}$, and $\alpha_{i,z}$ values for the carbon atom in polar environments can be

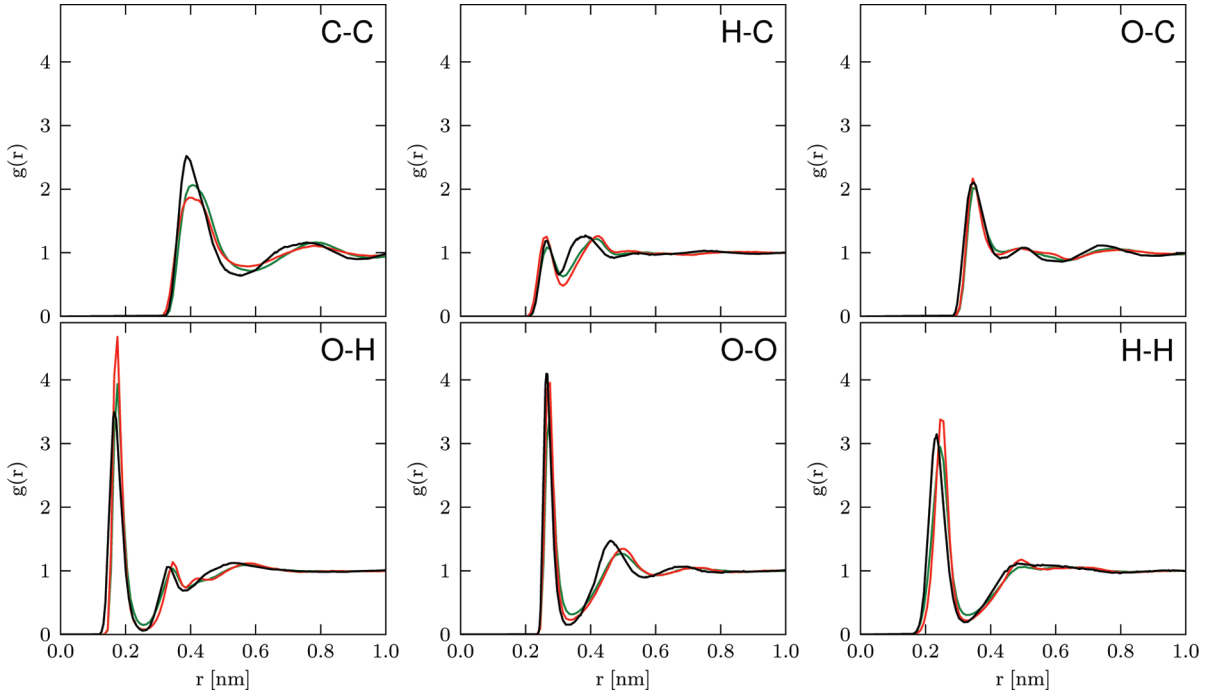

Figure 8. Radial distribution functions $g(r)$ for pairs of atoms involving the carbon (C), oxygen (O), and hydroxyl hydrogen (H) atoms of methanol in the pure liquid, obtained from simulations using the CPC (in green) and COS/M (in red) models. Experimental values are given as well (in black, taken from refs 81 and 82).

dx.doi.org/10.1021/ct300085z | J. Chem. Theory Comput. 2012, 8, 3839−3853

explained by the strong polarization of the methanol solute due to (hydrogen-bonding) interactions involving its hydroxyl group (instead of its methyl group) and the resulting intramolecular polarization. This may also offer an explanation for the need of using a low atomic polarizability for the carbon atom in condensed-phase systems (when compared to the gas phase estimate of α_C) to prevent molecular overpolarization effects. This need is illustrated by the distributions of α_C values that are scattered such that mean values were found well below the gas-phase estimate.

On the basis of the integration of Gaussian curves fitted to the distributions of obtained α_i values for the oxygen and carbon atoms in the water and methanol solutes, we obtained "optimal" values for α_O of 1.1×10^{-3} nm^3 both for water and methanol and of 1.1×10^{-3} nm^3 for methanol's α_C. These values are close to the effective values for atomic polarizabilities typically used for polarizable water and methanol models. The use of different combinations of solute or solvent force-field parameter sets in our simulations to generate the solvent configurations for use in the QM/MM calculations was not found to significantly affect these results. The obtained optimal value for α_O was used (together with the gas-phase estimate of partial charges) to parametrize a charge-on-spring (or Drude oscillator) based polarizable united-atom force field for methanol. Because of the wide spread in fitted α_C values, α_C was still treated as an effective, variable parameter in the parametrization procedure. The final model (designated as CPC) reproduces experimental data for thermodynamic properties of the pure liquid, as well as the mixing and solvation properties of methanol in water and chloroform. For this purpose, no special van der Waals parameters had to be introduced for interactions with the polar or apolar solvents considered.

AUTHOR INFORMATION

Corresponding Author

*E-mail: d.p.geerke@vu.nl.

Notes

The authors declare no competing financial interest.

ACKNOWLEDGMENTS

The authors thank Dr. Alan Soper for providing the experimental $g(r)$ data for liquid methanol. Financial support from the Netherlands Organisation for Scientific Research (NWO VENI grant 700.59.406) and from the Swiss National Science Foundation (SNF Fellowship for Prospective Researchers, grant PBEZP3-122915) is gratefully acknowledged.

DEDICATION

This work is dedicated to professor Wilfred F. van Gunsteren on the occasion of his 65th birthday.

REFERENCES

(1) Frenkel, D.; Smit, B. *Understanding Molecular Simulation*; Elsevier: San Diego, CA, 2002.

(2) van Gunsteren, W. F.; Bakowies, D.; Baron, R.; Chandrasekhar, I.; Christen, M.; Daura, X.; Gee, P.; Geerke, D. P.; Glaettli, A.; Huenenberger, P. H.; Kastenholz, M. A.; Ostenbrink, C.; Schenk, M.; Trzesniak, D.; van der Vegt, N. F. A.; Yu, H. B. Biomolecular modeling: Goals, problems, perspectives. *Angew. Chem., Int. Ed.* **2006**, *45*, 4064−4092.

(3) Dror, R. O.; Jensen, M.; Borhani, D. W.; Shaw, D. E. Exploring atomic resolution physiology on a femtosecond to millisecond timescale using molecular dynamics simulations. *J. Gen. Physiol.* **2010**, *135*, 555−562.

(4) Voelz, V. A.; Bowman, G. R.; Beauchamp, K.; Pande, V. S. Molecular simulation of ab initio protein folding for a millisecond folder NTL9(1−39). *J. Am. Chem. Soc.* **2010**, *132*, 1526−1528.

(5) Miao, L.; Schulten, K. Probing a structural model of the nuclear pore complex channel through molecular dynamics. *Biophys. J.* **2010**, *98*, 1658−1667.

(6) Dror, R. O.; Arlow, D. H.; Maragakis, P.; Mildorf, T. J.; Pan, A. C.; Xu, H.; Borhani, D. W.; Shaw, D. E. Activation mechanism of the beta(2)-adrenergic receptor. *Proc. Natl. Acad. Sci. U.S.A.* **2011**, *108*, 18684−18689.

(7) Hünenberger, P. H.; van Gunsteren, W. F. *Computer Simulation of Biomolecular Systems, Theoretical and Experimental Applications*; Kluwer Academic Publisher: Dordrecht, the Netherlands, 1997; Vol. 3.

(8) MacKerell, A. D. Empirical force fields for biological macromolecules: Overview and issues. *J. Comput. Chem.* **2004**, *25*, 1584−1604.

(9) Yu, H. B.; van Gunsteren, W. F. Accounting for polarization in molecular simulation. *Comput. Phys. Commun.* **2005**, *172*, 69−85.

(10) Cornell, W. D.; Cieplak, P.; Bayly, C. I.; Gould, I. R.; Merz, K. M.; Ferguson, D. M.; Spellmeyer, D. C.; Fox, T.; Caldwell, J. W.; Kollman, P. A. A second generation force field for the simulation of proteins, nucleic acids, and organic molecules. *J. Am. Chem. Soc.* **1995**, *117*, 5179−5197.

(11) Wang, J.; Wolf, R.; Caldwell, J.; Kollman, P.; Case, D. Development and testing of a general amber force field. *J. Comput. Chem.* **2004**, *25*, 1157−1174.

(12) Yang, L.; Tan, C.; Hsieh, M.; Wang, J.; Duan, Y.; Cieplak, P.; Caldwell, J.; Kollman, P.; Luo, R. New-generation amber united-atom force field. *J. Phys. Chem. B* **2006**, *110*, 13166−13176.

(13) MacKerell, A. D.; Bashford, D.; Bellott, M.; Dunbrack, R. L.; Evanseck, J. D.; Field, M. J.; Fischer, S.; Gao, J.; Guo, H.; Ha, S.; Joseph-McCarthy, D.; Kuchnir, L.; Kuczera, K.; Lau, F.; Mattos, C.; Michnick, S.; Ngo, T.; Nguyen, D. T.; Prodhom, B.; Reiher, W. E.; Roux, B.; Schlenkrich, M.; Smith, J. C.; Stote, R.; Straub, J.; Watanabe, M.; Wiorkiewicz-Kuczera, J.; Yin, D.; Karplus, M. All-atom empirical potential for molecular modeling and dynamics studies of proteins. *J. Phys. Chem. B* **1998**, *102*, 3586−3616.

(14) MacKerell, A. D.; Banavali, N.; Foloppe, N. Development and current status of the CHARMM force field for nucleic acids. *Biopolymers* **2000**, *56*, 257−265.

(15) Vanommeslaeghe, K.; Hatcher, E.; Acharya, C.; Kundu, S.; Zhong, S.; Shim, J.; Darian, E.; Guvench, O.; Lopes, P.; Vorobyov, I.; MacKerell, A. D. CHARMM general force field: A force field for drug-like molecules compatible with the CHARMM all-atom additive biological force fields. *J. Comput. Chem.* **2010**, *31*, 671−690.

(16) Jorgensen, W. L.; Tirado-Rives, J. The OPLS [optimized potentials for liquid simulations] potential functions for proteins, energy minimizations for crystals of cyclic peptides and crambin. *J. Am. Chem. Soc.* **1988**, *110*, 1657−1666.

(17) Jorgensen, W. L.; Maxwell, D. S.; Tirado-Rives, J. Development and testing of the OPLS all-atom force field on conformational energetics and properties of organic liquids. *J. Am. Chem. Soc.* **1996**, *118*, 11225−11236.

(18) Kaminski, G. A.; Friesner, R. A.; Tirado-Rives, J.; Jorgensen, W. L. Evaluation and reparametrization of the OPLS-AA force field for proteins via comparison with accurate quantum chemical calculations on peptides. *J. Phys. Chem. B* **2001**, *105*, 6474−6487.

(19) van Gunsteren, W. F.; Billeter, S. R.; Eising, A. A.; Hünenberger, P. H.; Krüger, P.; Mark, A. E.; Scott, W. R. P.; Tironi, I. G. *Biomolecular Simulation: The GROMOS96 Manual and User Guide*; vdf Hochschulverlag, ETH: Zurich, Switzerland, 1996.

(20) Oostenbrink, C.; Villa, A.; Mark, A. E.; van Gunsteren, W. F. A biomolecular force field based on the free enthalpy of hydration and solvation: The GROMOS force-field parameter sets 53A5 and 53A6. *J. Comput. Chem.* **2004**, *25*, 1656−1676.

(21) Schmid, N.; Eichenberger, A. P.; Choutko, A.; Riniker, S.; Winger, M.; Mark, A. E.; van Gunsteren, W. F. Definition and testing

of the GROMOS force-field versions 54A7 and 54B7. *Eur. Biophys. J.* **2011**, *40*, 843−856.
(22) Geerke, D. P.; van Gunsteren, W. F. Calculation of the free energy of polarization: Quantifying the effect of explicitly treating electronic polarization on the transferability of force-field parameters. *J. Phys. Chem. B* **2007**, *111*, 6425−6436.
(23) van Maaren, P. J.; van der Spoel, D. Molecular dynamics simulations of water with novel shell-model potentials. *J. Phys. Chem. B* **2001**, *105*, 2618−2626.
(24) Harder, E.; Anisimov, V. M.; Whitfield, T. W.; MacKerell, A. D.; Roux, B. Understanding the dielectric properties of liquid amides from a polarizable force field. *J. Phys. Chem. B* **2008**, *112*, 3509−3521.
(25) Warshel, A.; Levitt, M. Theoretical studies of enzymic reactions - dielectric, electrostatic and steric stabilization of carbonium-ion in reaction of lysozyme. *J. Mol. Biol.* **1976**, *103*, 227−249.
(26) Vesely, F. N-particle dynamics of polarizable stockmayer-type molecules. *J. Comput. Phys.* **1977**, *24*, 361−371.
(27) van Belle, D.; Couplet, I.; Prevost, M.; Wodak, S. J. Calculations of electrostatic properties in proteins - Analysis of contributions from induced protein dipoles. *J. Mol. Biol.* **1987**, *198*, 721−735.
(28) Drude, P. *The Theory of Optics*; Longmans, Green and Co.: New York, 1902.
(29) Straatsma, T. P.; McCammon, J. A. Molecular dynamics simulations with interaction potentials including polarization development of a noniterative method and application to water. *Mol. Simul.* **1990**, *5*, 181−192.
(30) Rappe, A. K.; Goddard, W. A. Charge equilibration for molecular-dynamics simulations. *J. Phys. Chem.* **1991**, *95*, 3358−3363.
(31) Rick, S. W.; Stuart, S. J.; Berne, B. J. Dynamical fluctuating charge force-fields - application to liquid water. *J. Chem. Phys.* **1994**, *101*, 6141−6156.
(32) Rick, S.; Stuart, S. In *Reviews in Computational Chemistry*; Lipkowitz, K. B., Boyd, D., Eds.; John Wiley Sons, Inc.: New Jersey, 2002; Vol. *18*.
(33) Caldwell, J. W.; Dang, L. X.; Kollman, P. A. Implementation of nonadditive intermolecular potentials by use of molecular-dynamics - development of a water water potential and water ion cluster interactions. *J. Am. Chem. Soc.* **1990**, *112*, 9144−9147.
(34) Yu, H. B.; Hansson, T.; van Gunsteren, W. F. Development of a simple, self-consistent polarizable model for liquid water. *J. Chem. Phys.* **2003**, *118*, 221−234.
(35) Sprik, M. Hydrogen-bonding and the static dielectric-constant in liquid water. *J. Chem. Phys.* **1991**, *95*, 6762−6769.
(36) van Belle, D.; Froeyen, M.; Lippens, G.; Wodak, S. Molecular-dynamics simulation of polarizable water by extended Lagrangian method. *Mol. Phys.* **1992**, *77*, 239−255.
(37) van Belle, D.; Wodak, S. J. Extended Lagrangian-formalism applied to temperature control and electronic polarization effects in molecular-dynamics simulations. *Comput. Phys. Commun.* **1995**, *91*, 253−262.
(38) Lamoureux, G.; Roux, B. Modeling induced polarization with classical Drude oscillators: Theory and molecular dynamics simulation algorithm. *J. Chem. Phys.* **2003**, *119*, 3025−3039.
(39) Miller, K. Calculation of the molecular polarizability tensor. *J. Am. Chem. Soc.* **1990**, *112*, 8543−8551.
(40) Applequist, J.; Carl, J. R.; Fung, K. K. Atom dipole interaction-model for molecular polarizability - application to polyatomic molecules - and determination of atom polarizabilities. *J. Am. Chem. Soc.* **1972**, *94*, 2952−2960.
(41) Anisimov, V. M.; Lamoureux, G.; Vorobyov, I. V.; Huang, N.; Roux, B.; MacKerell, A. D. Determination of electrostatic parameters for a polarizable force field based on the classical Drude oscillator. *J. Chem. Theory Comput.* **2005**, *1*, 153−168.
(42) Lamoureux, G.; MacKerell, A. D.; Roux, B. A simple polarizable model of water based on classical Drude oscillators. *J. Chem. Phys.* **2003**, *119*, 5185−5197.
(43) Geerke, D. P.; Van Gunsteren, W. F. The performance of non-polarizable and polarizable force-field parameter sets for ethylene glycol in molecular dynamics simulations of the pure liquid and its aqueous mixtures. *Mol. Phys.* **2007**, *105*, 1861−1881.
(44) Anisimov, V. M.; Vorobyov, I. V.; Roux, B.; MacKerell, A. D. Polarizable empirical force field for the primary and secondary alcohol series based on the classical drude model. *J. Chem. Theory Comput.* **2007**, *3*, 1927−1946.
(45) Caldwell, J. W.; Kollman, P. A. Structure and properties of neat liquids using nonadditive molecular-dynamics - water, methanol, and n-methylacetamide. *J. Phys. Chem.* **1995**, *99*, 6208−6219.
(46) Gao, J. L.; Habibollazadeh, D.; Shao, L. A polarizable intermolecular potential function for simulation of liquid alcohols. *J. Phys. Chem.* **1995**, *99*, 16460−16467.
(47) Dang, L. X.; Chang, T. M. Many-body interactions in liquid methanol and its liquid/vapor interface: A molecular dynamics study. *J. Chem. Phys.* **2003**, *119*, 9851−9857.
(48) Patel, S.; Brooks, C. L. A nonadditive methanol force field: Bulk liquid and liquid-vapor interfacial properties via molecular dynamics simulations using a fluctuating charge model. *J. Chem. Phys.* **2005**, *122*, 024508.
(49) Schropp, B.; Tavan, P. The polarizability of point-polarizable water models: Density functional theory molecular mechanics results. *J. Phys. Chem. B* **2008**, *112*, 6233−6240.
(50) Kunz, A.-P. E.; van Gunsteren, W. F. Development of a nonlinear classical polarization model for liquid water and aqueous solutions: COS/D. *J. Phys. Chem. A* **2009**, *113*, 11570−11579.
(51) Ren, P. Y.; Ponder, J. W. Consistent treatment of inter- and intramolecular polarization in molecular mechanics calculations. *J. Comput. Chem.* **2002**, *23*, 1497−1506.
(52) Ren, P. Y.; Wu, C.; Ponder, J. W. Polarizable atomic multipole-based molecular mechanics for organic molecules. *J. Chem. Theory Comput.* **2011**, *7*, 3143−3161.
(53) Thole, B. Molecular polarizabilities calculated with a modified dipole interaction. *Chem. Phys.* **1981**, *59*, 341−350.
(54) Baker, C. M.; MacKerell, A. D. Polarizability rescaling and atom-based Thole scaling in the CHARMM Drude polarizable force field for ethers. *J. Mol. Model.* **2010**, *16*, 567−576.
(55) Yu, H. B.; Geerke, D. P.; Liu, H. Y.; van Gunsteren, W. F. Molecular dynamics simulations of liquid methanol and methanol-water mixtures with polarizable models. *J. Comput. Chem.* **2006**, *27*, 1494−1504.
(56) Becke, A. D. Density-functional thermochemistry. 3. The role of exact exchange. *J. Chem. Phys.* **1993**, *98*, 5648−5652.
(57) Stephens, P. J.; Devlin, F. J.; Cabalowski, C. F.; Frisch, M. J. Ab-initio calculation of vibrational absorption and circular-dichroism spectra using density-functional force-fields. *J. Phys. Chem.* **1994**, *98*, 11623−11627.
(58) Hertwig, R. H.; Koch, W. On the parameterization of the local correlation functional. What is Becke-3-LYP? *Chem. Phys. Lett.* **1997**, *268*, 345−351.
(59) Kendall, R. A.; Dunning, T. H.; Harrison, R. J. Electron-affinities of the 1s-row atoms revisited - systematic basis-sets and wave-functions. *J. Chem. Phys.* **1992**, *96*, 6796−680.
(60) Schmidt, M. W.; Baldridge, K. K.; Boatz, J. A.; Elbert, S. T.; Gordon, M. S.; Jensen, J. H.; Koseki, S.; Matsunaga, N.; Nguyen, K. A.; Su, S. J.; Windus, T. L.; Dupuis, M.; Montgomery, J. A. General atomic and molecular electronic-structure system. *J. Comput. Chem.* **1993**, *14*, 1347−1363.
(61) Gordon, M.; Schmidt, M. In *Theory and Applications of Computational Chemistry: The First Forty Years*; Dykstra, C., Frenking, G., Kim, K., Scuseria, G., Eds.; Elsevier: Amsterdam, 2005.
(62) Berendsen, H. J. C.; Postma, J. P. M.; van Gunsteren, W. F.; Hermans, J. In *Intermolecular Forces*; Reidel: Dordrecht, The Netherlands, 1981; pp 331−338.
(63) Berendsen, H. J. C.; Grigera, J. R.; Straatsma, T. P. The missing term in effective pair potentials. *J. Phys. Chem.* **1987**, *91*, 6269−6271.
(64) Walser, R.; Mark, A. E.; van Gunsteren, W. F.; Lauterbach, M.; Wipff, G. The effect of force-field parameters on properties of liquids: Parametrization of a simple three-site model for methanol. *J. Chem. Phys.* **2000**, *112*, 10450−10459.

(65) Weerasinghe, S.; Smith, P. E. A Kirkwood-Buff derived force field for methanol and aqueous methanol solutions. *J. Phys. Chem. B* **2005**, *109*, 15080−15086.
(66) Tironi, I. G.; van Gunsteren, W. F. A molecular-dynamics simulation study of chloroform. *Mol. Phys.* **1994**, *83*, 381−403.
(67) Hockney, R. W. The potential calculation and some applications. *Methods Comput. Phys.* **1970**, *9*, 136−211.
(68) Berendsen, H. J. C.; Postma, J. P. M; van Gunsteren, W. F.; Di Nola, A.; Haak, J. R. Molecular-dynamics with coupling to an external bath. *J. Chem. Phys.* **1984**, *81*, 3684−3690.
(69) Ryckaert, J.-P.; Ciccotti, G.; Berendsen, H. Numerical integration of the cartesian equations of motion of a system with constraints: Molecular dynamics of n-alkanes. *J. Comput. Phys.* **1977**, *23*, 327−341.
(70) Tironi, I. G.; Sperb, R.; Smith, P. E.; van Gunsteren, W. F. A generalized reaction field method for molecular dynamics simulations. *J. Chem. Phys.* **1995**, *102*, 5451−5495.
(71) Heinz, T. N.; van Gunsteren, W. F.; Hunenberger, P. H. Comparison of four methods to compute the dielectric permittivity of liquids from molecular dynamics simulations. *J. Chem. Phys.* **2001**, *115*, 1125−1136.
(72) Singh, U.; Kollman, P. An approach to computing electrostatic charges for molecules. *J. Comput. Chem.* **1984**, *5*, 129−145.
(73) de Proft, F.; Tielens, F.; Geerlings, P. Performance and basis set dependence of density functional theory dipole and quadrupole moments. *THEOCHEM* **2000**, *506*, 1−8.
(74) Johnson, R. D., III. *NIST Standard Reference Database*, number 101, release 15b; National Institute of Standards and Technology: Gaithersburg, MD, August 2011.
(75) Geerke, D. P.; van Gunsteren, W. F. On the calculation of atomic forces in classical simulation using the charge-on-spring method to explicitly treat electronic polarization. *J. Chem. Theory Comput.* **2007**, *3*, 2128−2137.
(76) Lide, D. R. *CRC Handbook of Chemistry and Physics*; CRC Press: Boca Raton, FL, 2007.
(77) Scott, W. R. P.; Hunenberger, P. H.; Tironi, I. G.; Mark, A. E.; Billeter, S. R.; Fennen, J.; Torda, A. E.; Huber, T.; Kruger, P.; van Gunsteren, W. F. The GROMOS biomolecular simulation program package. *J. Phys. Chem. A* **1999**, *103*, 3596−3607.
(78) Lin, Z.; Kunz, A.; van Gunsteren, W. F. A one-site polarizable model for liquid chloroform: COS/C. *Mol. Phys.* **2010**, *108*, 1749−1757.
(79) Yu, H. B.; van Gunsteren, W. F. Charge-on-spring polarizable water models revisited: From water clusters to liquid water to ice. *J. Chem. Phys.* **2004**, *121*, 9549−9564.
(80) Glättli, A.; Daura, X.; van Gunsteren, W. F. Derivation of an improved simple point charge model for liquid water: SPC/A and SPC/L. *J. Chem. Phys.* **2002**, *116*, 9811−9828.
(81) Yamaguchi, T.; Hidaka, K.; Soper, A. The structure of liquid methanol revisited: A neutron diffraction experiment at −80 degrees C and +25 degrees C. *Mol. Phys.* **1999**, *96*, 1159−1168.
(82) Yamaguchi, T.; Hidaka, K.; Soper, A. The structure of liquid methanol revisited: a neutron diffraction experiment at −80 degrees C and +25 degrees C. *Mol. Phys.* **1999**, *97*, 603−605.
(83) Lama, R. F.; Lu, C. Y. Excess thermodynamic properties of aqueous alcohol solutions. *J. Chem. Eng. Data* **1965**, *10*, 216−219.
(84) Guillot, B. A reappraisal of what we have learnt during three decades of computer simulations on water. *J. Mol. Liq.* **2002**, *101*, 219−260.
(85) Fernández, D. P.; Mulev, Y.; Goodwin, A. R. H.; Levelt Sengers, J. M. H. A database for the static dielectric constant of water and steam. *J. Phys. Chem.* **1995**, *24*, 33−70.
(86) Dang, L. The nonadditive intermolecular potential for water revised. *J. Chem. Phys.* **1992**, *97*, 2659−2660.
(87) Smith, D.; Dang, L. Computer simulations of NaCl association in polarizable water. *J. Chem. Phys.* **1994**, *100*, 3757−3766.
(88) Stern, H.; Rittner, F.; Berne, B.; Friesner, R. Combined fluctuating charge and polarizable dipole models: Application to a five-site water potential function. *J. Chem. Phys.* **2001**, *115*, 2237−2251.
(89) Lamoureux, G.; Harder, E.; Vorobyov, I. V.; Roux, B.; MacKerell, A. D. A polarizable model of water for molecular dynamics simulations of biomolecules. *Chem. Phys. Lett.* **2006**, *418*, 245−249.
(90) Vorobyov, I. V.; Anisimov, V. M.; MacKerell, A. D. Polarizable empirical force field for alkanes based on the classical drude oscillator model. *J. Phys. Chem. B* **2005**, *109*, 18988−18999.
(91) Foloppe, N.; MacKerell, A. D. All-atom empirical force field for nucleic acids: I. Parameter optimization based on small molecule and condensed phase macromolecular target data. *J. Comput. Chem.* **2000**, *21*, 86−104.
(92) Mikhail, S. Z.; Kimel, W. R. Densities and viscosities of methanol-water mixtures. *J. Chem. Eng. Data* **1961**, *6*, 533−537.
(93) McClellan, A. L. L. *Tables of Experimental Dipole Moments*; Rahara Enterprise: El Cerrito, CA, 1989.
(94) Hurle, R. L.; Easteal, A. J.; Woolf, L. A. Self-diffusion in monohydric alcohols under pressure. Methanol, methan(2H)ol and ethanol. *J. Chem. Soc., Faraday Trans. 1* **1985**, *81*, 769−779.
(95) Katritzky, A. R.; Oliferenko, A. A.; Oliferenko, P. V.; Petrukhin, R.; Tatham, D. B.; Maran, U.; Lomaka, A.; Acree, W. E. A general treatment of solubility. 1. The QSPR correlation of solvation free energies of single solutes in series of solvents. *J. Chem. Inf. Comput. Sci.* **2003**, *43*, 1794−1805.